Electronic Supplementary Material (ESI) for Analytical Methods.

Supporting Information

Suppressor and calibration standard limitations in cation chromatography of ammonium and 10 alkylamines in atmospheric samples

Leyla Salehpoor and Trevor C. VandenBoer*

Department of Chemistry, York University, Toronto, ON, Canada.

*Correspondence to: tvandenb@yorku.ca

S1. Chromeleon data file of the final optimized cation separation method

The final optimized ion chromatographic method was developed using the script editor in Chromeleon to separate and quantify ten alkylamines and six inorganic cations. The highest selectivity and separation efficiency were achieved using 4 µm packed columns and resin-based suppressors. In this method, the MSA gradient was from 1-8 mM with a flow rate of 1.25 mL min^{-1} at 55 °C, a total run time of 35 mins. Analytes were passed through a suppressor in stepped-legacy external water mode with a current of 4-30 mA before detection in the conductivity detector (Fig. S1).

```
{Initial Time}          Instrument Setup
            DC.Compartment_TC.AcquireExclusiveAccess
            DC.Column_TC.AcquireExclusiveAccess
            DC.Suppressor1.PowerMode                    Legacy
            Sampler.DelayVolume                         125 [µl]
            Sampler.FlushFactor                         1
            Sampler.DeliverSpeed                        1.0 [ml/min]
            Pump_1.Degasser                             Off
            DC.Suppressor1.OtherEluent                  0.0 [mN]
            Pump_1.Pressure.UpperLimit                  4500 [psi]
            Pump_1.%A.Equate                            "%A Water"
            Pump_1.Pressure.LowerLimit                  300 [psi]
            Pump_1.%B.Equate                            "%B 100 mM NaOH"
            Pump_1.%C.Equate                            "%C 20 mM MSA"
            Pump_1.%D.Equate                            "%D Water"
            DC.Column_TC.Mode                           On
            DC.Column_TC.TemperatureSet                 55.00 [°C]
            DC.Compartment_TC.Mode                      On
            DC.Compartment_TC.TemperatureSet            15.00 [°C]
            DC.Suppressor1.Type CDRS_4mm
            DC.Suppressor1.H2SO4                        0.0 [mM]
            DC.Suppressor1.MSA                          1.0 [mM]
            DC.Suppressor1.RecommendedCurrent           4 [mA]
            DC.Suppressor1.CurrentSet                   4 [mA]
            CDet1.Rise_Time                             0.50 [s]
            CDet1.Data_Collection_Rate                  10.0 [Hz]
            CDet1.CellHeater.Mode                       On
            CDet1.CellHeater.TemperatureSet             35.00 [°C]
            CDet1.Temperature_Compensation              1.7 [%/°C]
            Sampler.InjectPosition
            Sampler.DeliverSample                       Volume=Bleed
            Sampler.DeliverRinse                        400,
Position=Rinse
            Sampler.LoadPosition
            Sampler.DeliverSample
            Sampler.EndSamplePrep
0.000       Inject
            Wait        Sampler.CycleTimeState,
Run=Hold,
Timeout=Infinite
            Sampler.Inject
0.000       Start Run
            Pump_1.Degasser                             On
            Pump_1.Pump_1_Pressure.AcqOn
            CDet1.CD_1.AcqOn
            CDet1.CD_1_Total.AcqOn
            CDet1.Autozero
0.000       Run                                         Duration = 35.000 [min]
```

	Pump_1.Flow	1.250 [ml/min]
	Pump_1.%B.Value	0.0 [%]
	Pump_1.%C.Value	5.0 [%]
	Pump_1.%D.Value	0.0 [%]
	Pump_1.Curve	5
5.000		
	Sampler.BeginOverlap	
18.000		
	Pump_1.Flow	1.250 [ml/min]
	Pump_1.%B.Value	0.0 [%]
	Pump_1.%C.Value	5.0 [%]
	Pump_1.%D.Value	0.0 [%]
	Pump_1.Curve	5
	DC.Suppressor1.CurrentSet	15 [mA]
20.000		
	Pump_1.Flow	1.250 [ml/min]
	Pump_1.%B.Value	0.0 [%]
	Pump_1.%C.Value	5.0 [%]
	Pump_1.%D.Value	0.0 [%]
	Pump_1.Curve	7
	Pump_1.Flow	1.250 [ml/min]
	Pump_1.%B.Value	0.0 [%]
	Pump_1.%C.Value	20.0 [%]
	Pump_1.%D.Value	0.0 [%]
	Pump_1.Curve	7
	DC.Suppressor1.CurrentSet	30 [mA]
25.000		
	Pump_1.Flow	1.250 [ml/min]
	Pump_1.%B.Value	0.0 [%]
	Pump_1.%C.Value	40.0 [%]
	Pump_1.%D.Value	0.0 [%]
	Pump_1.Curve	7
30.000		
	Pump_1.Flow	1.250 [ml/min]
	Pump_1.%B.Value	0.0 [%]
	Pump_1.%C.Value	40.0 [%]
	Pump_1.%D.Value	0.0 [%]
	Pump_1.Curve	5
	Pump_1.Flow	1.250 [ml/min]
	Pump_1.%B.Value	0.0 [%]
	Pump_1.%C.Value	5.0 [%]
	Pump_1.%D.Value	0.0 [%]
	Pump_1.Curve	5
	DC.Suppressor1.CurrentSet	30 [mA]
34.000		
	Pump_1.Flow	1.250 [ml/min]
	Pump_1.%B.Value	0.0 [%]
	Pump_1.%C.Value	5.0 [%]
	Pump_1.%D.Value	0.0 [%]
	Pump_1.Curve	5
	DC.Suppressor1.CurrentSet	4 [mA]
35.000	Stop Run	
	Pump_1.Pump_1_Pressure.Acq	Off
	CDet1.CD_1.Acq	Off
	CDet1.CD_1_Total.Acq	Off
35.000	Post Run	Duration = 0.000 [min]
	DC.Column_TC.ReleaseExclusiveAccess	
	DC.Compartment_TC.ReleaseExclusiveAccess	
End		

Fig. S1 Chromeleon method data file at optimum gradient method with mobile phase flow rate of 1.25 mL min^{-1} at 55 ºC and suppressor stepped-legacy mode.

S2. Statistical approaches to evaluate the significance of the y-intercept

There are three different statistical approaches to evaluate the significance of the y-intercept value (Table S1 and S2).[1,2] The first approach considers the null hypothesis by equating the y-intercept to zero (H_0: b = 0) at the 95% confidence interval and this hypothesis is evaluated based on the Student's test statistic or *p*-value. The null hypothesis is accepted when the t-statistic < t-critical value or *p*-value > 0.05. This statistically proves that the y-intercept is not significantly different from zero and a calibration curve can be forced through the origin. Next, the confidence interval (CI) of the y-intercept can be calculated by using equation E1.

$$CI = b \pm t \times SE_b \quad \text{(E1)}$$

where b is the y-intercept, t is the Student's t-value (degree of freedom = n – 2), and SE_b is the standard error of the y-intercept. If the obtained value spans zero, the y-intercept is not significantly different from zero. Finally, by comparing the b with SE_b: if $b > SE_b$ then the intercept value is significant but if $b \leq SE_b$ then the intercept is insignificant, and a calibration curve can be statistically justified to be forced through the origin.

Table S1: Three different statistical approaches to check significance of intercept value of inorganic cation standards.

Cation	t-statistic 95% CI	t-critical (LC–UC)*	*P*-value	CI of b	b ± SE_b
Li^+	-1.728	-0.125–0.029	0.159	-0.125–0.029	-0.048 ± 0.028
Na^+	-1.611	-0.135–0.036	0.182	-0.135–0.036	-0.050 ± 0.031
K^+	-1.938	-0.280–0.050	0.125	-0.280–0.050	-0.115 ± 0.059

***LC and UC stand for lower critical and upper critical values in t-critical.**

Table S2: Results of statistical approaches to accept or reject the significance of intercept value of inorganic cation standards.

Cation	t-statistic < t-critical	*P*-value > 0.05	Zero includes in CI of b	b ≤ SE_b
Li^+	✓	✓	✓	X
Na^+	✓	✓	✓	X
K^+	✓	✓	✓	X
	H_0: b = 0	**H_0: b = 0**	**H_0: b = 0**	**H_1: b ≠ 0**

S3. The impact of temperature on the separation of inorganic cations and alkylamines

The effect of elevated temperature on the analytical column across the range of 45 °C to 55 °C resulted in enhanced selectivity, chromatographic peak shape, and separation efficiency when separating ten alkylamines and four inorganic cations in dynamic recycled water mode (Fig. S2).

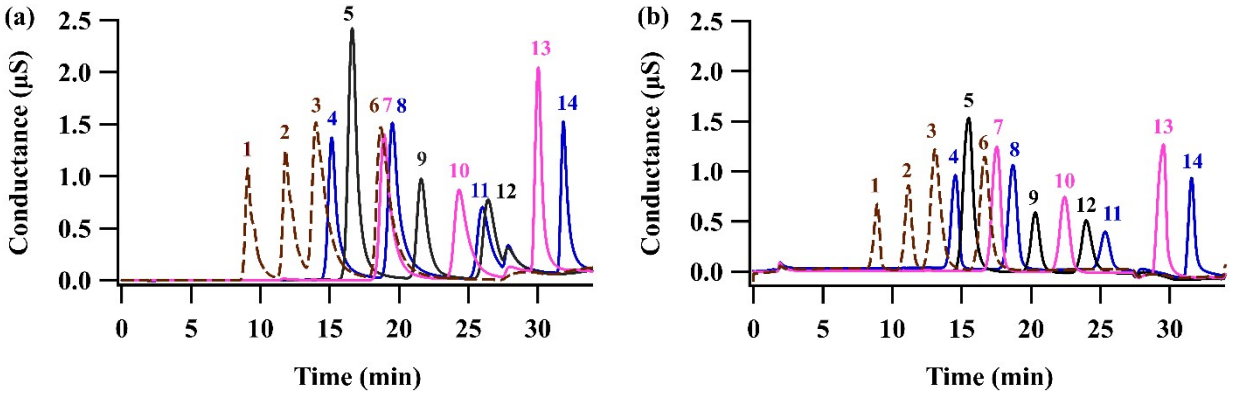

Fig. S2 Separation of inorganic cations and three amine mixtures with an MSA gradient from 1- 8 mM and flow rate of 1.25 mL min^{-1} at (a) 45 °C and (b) 55 °C. Analytes were passed through a suppressor in dynamic recycled water mode before detection. Inorganic cations and three amine mixtures are coloured separately: dashed trace (inorganic cations), blue solid trace ($MEtAH^+$, $DMAH^+$, $DEAH^+$, $TEAH^+$), black solid trace ($MMAH^+$, $iMPAH^+$, $TMAH^+$), and pink solid trace ($MEAH^+$, $MPAH^+$, $MBAH^+$). The identity, numeric order of elution, and mass of each cation separated are: Li^+ (1, 74 ng), Na^+ (2, 296 ng), NH_4^+ (3, 374 ng), $MEtAH^+$ (4, 991 ng), $MMAH^+$ (5, 358 ng), K^+ (6, 743 ng), $MEAH^+$ (7, 567 ng), $DMAH^+$ (8, 356 ng), $iMPAH^+$ (9, 684 ng), $MPAH^+$ (10, 712 ng), $DEAH^+$ (11, 703 ng), $TMAH^+$ (12, 326 ng), $MBAH^+$ (13, 736 ng), and $TEAH^+$ (14, 718 ng).

S4. Stability of amine standards over time

Instrumental sensitivities of amines prepared in DIW and MSA were measured over 90 days with three different suppressor modes: dynamic recycle, stepped-legacy recycle, and stepped-legacy external water (Fig. S3). The decay rate of amines (day^{-1}) was measured by plotting natural logarithm of the normalized amine sensitivities relative to K^+ versus their age in days in both DIW and MSA to investigate the effect of volatilization on the amine loss mechanism. Figure S4 illustrates the decay rate of iMPA at different suppressor modes. Also, relative effective volatilities of amines ($K_{eff} = K_a/K_H$) were calculated (Table S3) to compare to the losses measured in both matrices over 90 days.

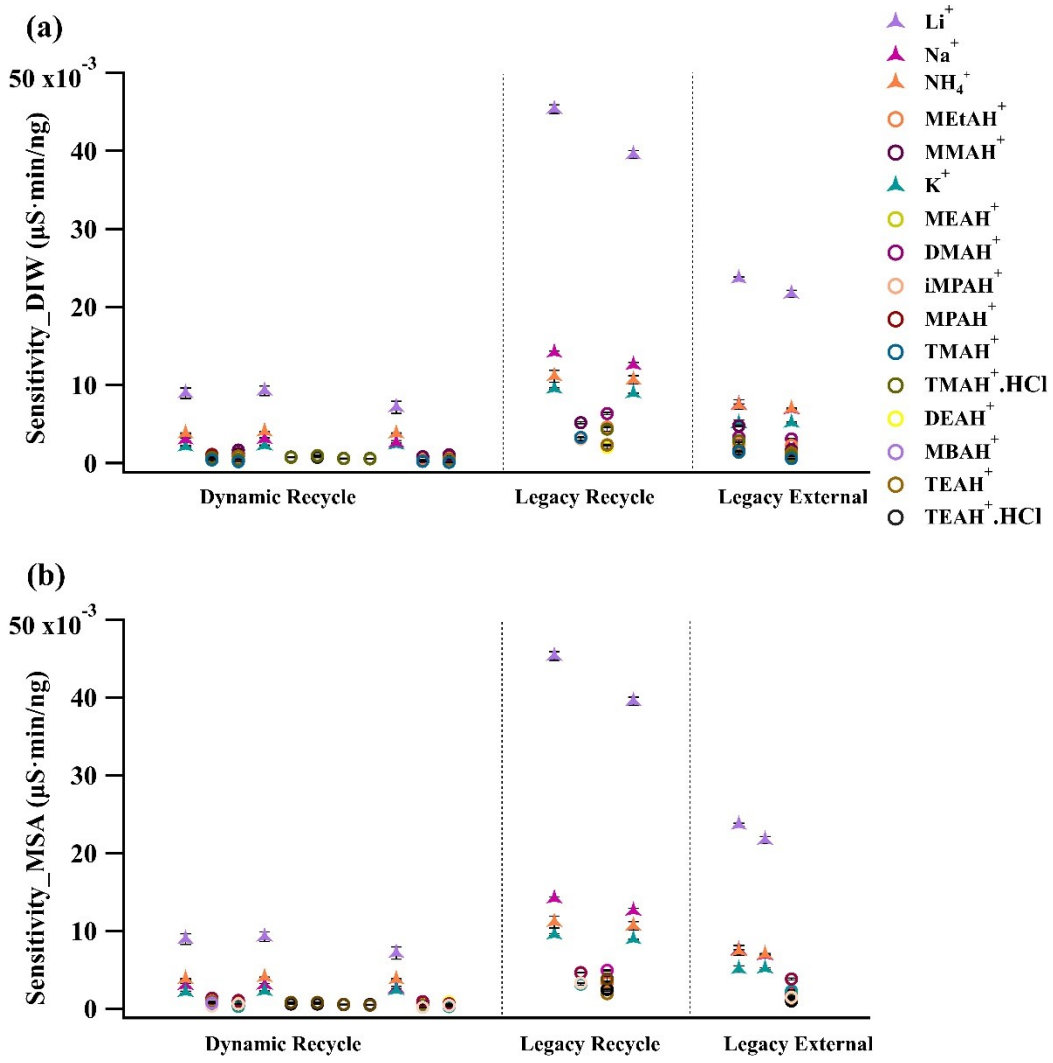

Fig. S3 Sensitivities of inorganic cations and alkylamines at different suppressor setups: dynamic recycle, stepped-legacy recycle, and stepped-legacy external water in (a) DIW and (b) MSA solutions.

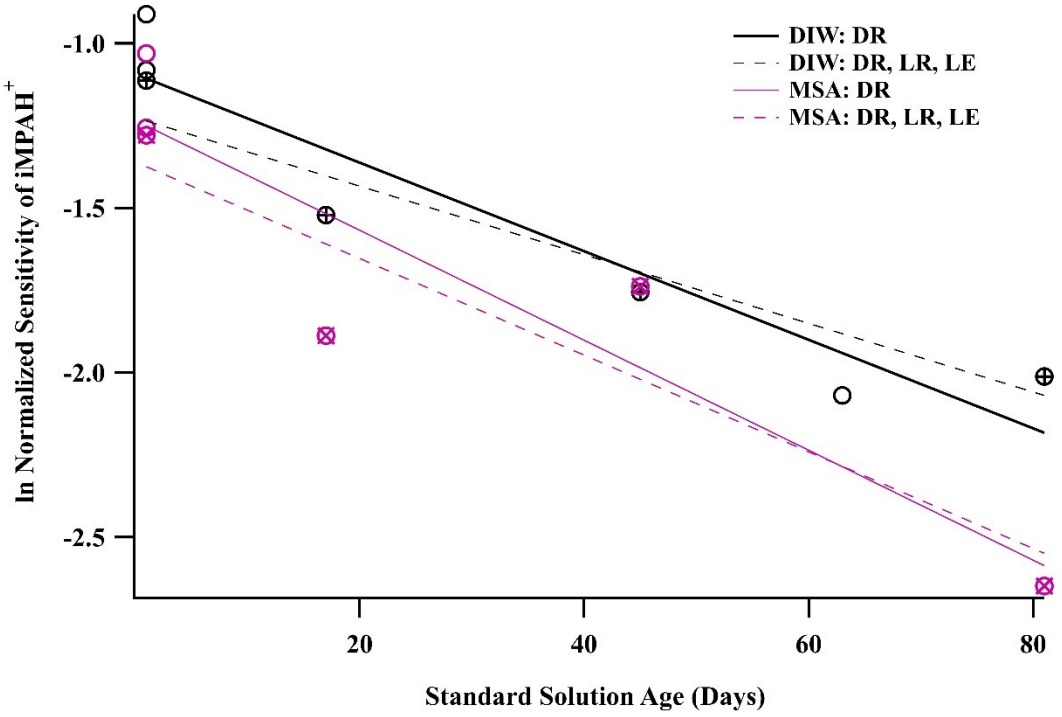

Fig. S4 The experimental loss rate of $iMPAH^+$ was determined by the slope of natural logarithm of normalized $iMPAH^+$ sensitivities with K^+ versus its age in day. The decay rate in DIW and MSA was 0.010 ± 0.002 (Day^{-1}; $r^2 = 0.917$) and 0.015 ± 0.005 (Day^{-1}; $r^2 = 0.819$), respectively, with suppressor in dynamic recycle mode. The decay rate with suppressor in three different modes: dynamic recycle (DR), stepped-legacy recycle (LR), and stepped-legacy external (LE) was measured 0.013 ± 0.002 (Day^{-1}; $r^2 = 0.903$) in DIW and 0.016 ± 0.003 (Day^{-1}; $r^2 = 0.855$) in MSA.

Table S3: Weak acid ionization constant (K_a), pKa, Henry's law constant (K_H), and the ratio of K_a-to-K_H of alkylamines at 298 K.

Amine	Formula	MW (g/mol)	PK_a	K_a	K_H (M atm^{-1})	K_a/K_H (atm M^{-1})
MEtA	$HOC_2H_4NH_2$	61.1	9.50	3.2×10^{-10}	6.1×10^{6}	5.2×10^{-17}
MMA	CH_3NH_2	31.1	10.66	2.2×10^{-11}	1.2×10^{2}	1.8×10^{-13}
MEA	$C_2H_5NH_2$	45.1	10.65	2.2×10^{-11}	8.0×10^{1}	2.8×10^{-13}
DMA	$(CH_3)_2NH$	45.1	10.73	1.9×10^{-11}	6.1×10^{1}	3.1×10^{-13}
iMPA	C_3H_9N	59.1	10.63	2.3×10^{-11}	2.2×10^{1}	1.1×10^{-12}
MPA	$C_3H_7NH_2$	59.1	10.54	2.9×10^{-11}	4.9×10^{1}	5.9×10^{-13}
TMA	$(CH_3)_3N$	59.1	9.80	1.6×10^{-10}	3.8	4.2×10^{-11}
DEA	$(C_2H_5)_2NH$	73.1	10.84	1.5×10^{-11}	1.8×10^{1}	8.0×10^{-13}
MBA	$C_4H_9NH_2$	73.1	10.60	2.5×10^{-11}	2.9×10^{1}	8.6×10^{-13}
TEA	$(C_2H_5)_3N$	101.2	10.75	1.8×10^{-11}	8.7	2.0×10^{-12}

S5. Calibration approaches of cation standards

The accuracy of linear calibration curves of inorganic cations was assessed using the R^2 values of calibration standards and RE % of both calibration standards and check standards compared to their known concentrations as an evaluation of accuracy. Figure S5 shows three different types of regression lines with corresponding RE%: (a,b) forced through (0,0), (c,d) not forced through origin but included (0,0) in the regression, and (e,f) not forced through the origin and not including (0,0). Metrics describing the performance of the optimized method for quantifying our full suite of cations are provided in Table S4.

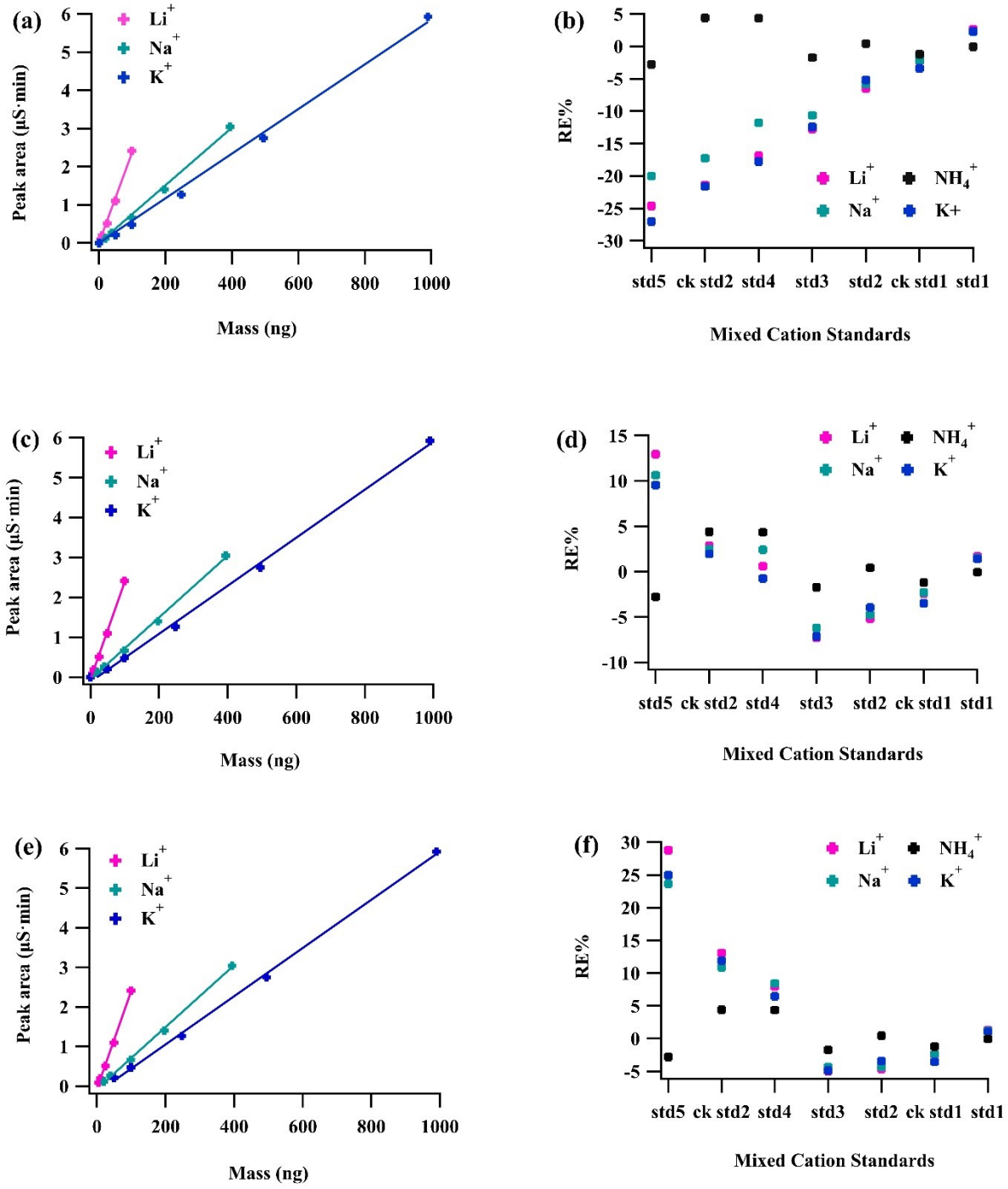

Fig. S5 Three different calibration curves of inorganic cations and RE % from both calibration standards (std) and check standards (ck std): (a) regression lines and (b) RE% by forcing to zero; (c) regression lines and (d) RE% not forcing to zero and including (0,0); (e) regression lines and (f) RE% not forcing to zero and excluding (0,0).

Table S4: Calibration standards and reagent blanks of inorganic cations and alkylamines were

used to analyze sensitivity (n = 5 inorganic cation, n = 3 amines), precision (n = 5 inorganic cation, n = 3 amines), accuracy (n = 5), and an average of LODs with ranges (n = 3). The suppressor was operated in stepped-legacy external water mode.

Cation	Sensitivity ($\mu S \cdot min\ mol^{-1}$)	Precision[1] (%)	Accuracy[2] (%)	Average LOD (nmol)	LOD range (nmol)
Li^+	1.61E08	7	97-98	0.20±0.01	0.19–0.21
Na^+	1.73E08	6	97-98	0.29±0.20	0.13–0.51
NH_4^+	1.32E08	4	95-99	0.17±0.12	0.09–0.31
$MEtAH^+$	1.60E08	7	82	0.13±0.01	0.11–0.14
$MMAH^+$	1.52E08	8	91	0.17±0.01	0.16–0.18
$MEAH^+$	1.48E08	13	87	0.21±0.003	0.21
K^+	2.17E08	8	97-98	0.17±0.05	0.13–0.22
$DMAH^+$	1.65E08	6	90	0.17±0.02	0.15–0.19
$iMPAH^+$	1.20E08	11	87	0.35±0.06	0.36–0.30
$MPAH^+$	1.55E08	8	83	0.22±0.03	0.20–0.25
$DEAH^+$	1.39E08	7	88	0.45±0.02	0.43–0.47
$TMAH^+$	1.07E08	11	85	0.43±0.06	0.36–0.43
$TMAH^+$.HCl	1.68E08	4	86	0.27±0.04	0.23–0.32
$MBAH^+$	1.55E08	11	80	0.13±0.02	0.12–0.15
$TEAH^+$	1.47E08	4	94	3.41±0.32	3.11–3.74
$TEAH^+$.HCl	1.60E08	4	94	1.68±0.16	1.54–1.85

[1] Precision was calculated using %RSD of the slope from replicate linear calibration curves for both inorganic cations and alkylamines.

[2] Accuracy was determined by calculating the %RE of the check standards selected from the upper and lower ranges (inorganic cations) and midpoints (alkylamines) of the calibration standards (Sections 2.4.2. and 2.4.3).

S6. Methods to optimize suppressor functionality

Suppressor cleaning with MSA (500 mM) and NaOH (200 mM) were each performed at a flow rate of 1.25 mL min^{-1} for 12 mins according to the manufacturer's instructions. The acid wash was intended here to dissolve $Mg(OH)_{2(s)}$ and $Ca(OH)_{2(s)}$ (R1; Ca^{2+} has the same salt formation equilibria) which were hypothesized to have been generated in the resin bed due to an excess of OH^- in the electrolytic channel when operating in recycled water mode, particularly where the applied current from the dynamic approach may have been over-suppressing the column effluent compared that required for the eluent strength (R2). The suppressor was then reconditioned using NaOH to resume normal operation.

$$Mg^{2+}_{(aq)} + 2OH^-_{(aq)} \rightleftharpoons Mg(OH)_{2(s)} \quad \text{(R1)}$$

$$Mg(OH)_{2(s)} + 2H_3O^+_{(aq)} \rightleftharpoons Mg^{2+}_{(aq)} + 4H_2O_{(l)} \quad \text{(R2)}$$

However, this acid and base treatment procedure did not recover sensitivity nor detection of Mg^{2+} and Ca^{2+} analytes once they were observed to start declining (Fig. S6). The suppressor was then changed from dynamic to stepped-legacy mode with the same recycled water supply, to reduce the possibility of prolonged over-suppression of the eluent compared to dynamic mode, particularly at the low initial 1 mM MSA concentrations which our optimized method holds for an extended period at the start of each run. The very low eluent strength conditions provide the needed selectivity to separate the target analytes. Using a new suppressor in stepped-legacy mode was used with the current changed to match the eluent programming, taking into account the solvent delay for the increased OH^- concentration to reach the suppressor. There was an improvement in analyte sensitivities, a reduction in the extent of loss for monovalent cations, and it was possible to detect Mg^{2+} and Ca^{2+} ions in ~ 100 samples. However, losses of alkylamines in the suppressor were persistent along with fatal damage to the suppressor after 2 months of operation. With the improved performance, the suppressor had the option to be cleaned with oxalic acid to restore suppression capability. In this cleanup procedure, the suppressor was flushed out with oxalic acid as an alternative to dissolve $Mg(OH)_{2(s)}$ and $Ca(OH)_{2(s)}$ that may have formed in the resin and remove them more effectively as MgC_2O_4 and CaC_2O_4. Unfortunately, the oxalic acid wash was found to only temporarily improve suppressor function, with the loss of Mg^{2+} and Ca^{2+} peaks reoccurred after running ~ 80 additional samples. Finally, the suppressor was switched to external water to prevent the degree to which intrusion and accumulation of column stationary phase

material and/or $Mg(OH)_{2(s)}$ and $Ca(OH)_{2(s)}$ were possible on the regenerant side of the electrolytic suppressor compartments (Fig. 1).

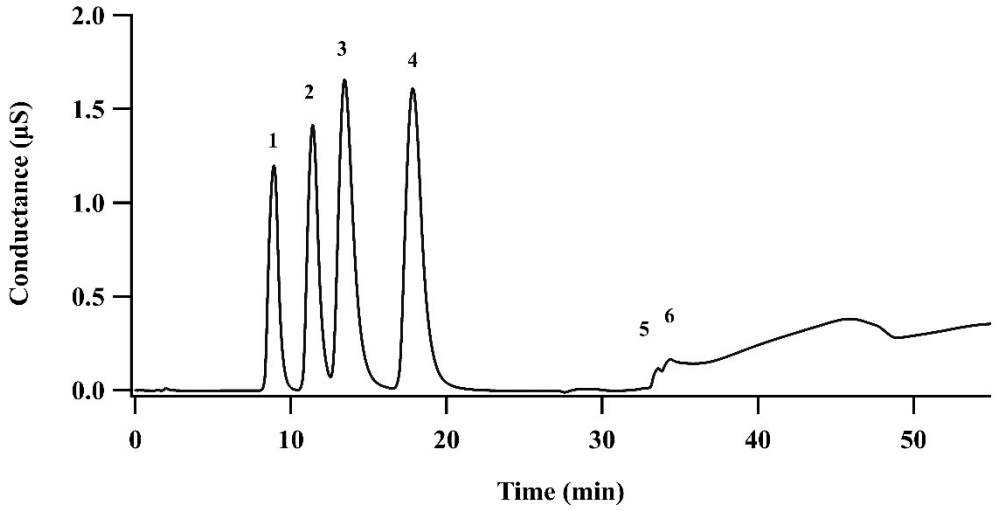

Fig. S6 Chromatogram of inorganic cations: Li^+ (1), Na^+ (2), NH_4^+ (3), K^+ (4), Mg^{2+} (5), and Ca^{2+} (6) to demonstrate the loss of Mg^{2+} and Ca^{2+} ions due to suppressor failure.

S7. Review of quantitative IC methods for inorganic cations

Over the past decade, ion chromatographic methods have been developed using H_3O^+ gradient methods to separate and quantify inorganic cations (Figure S7). Various cation-exchange columns and suppressors were utilized in these methods, such as CS12A (8.5 µm) and CSRS 300, CS17 (7 µm) and CSRS 300, CS19 (5.5 µm) and CERS 500, and CS19 (4 µm) and CDRS 600.

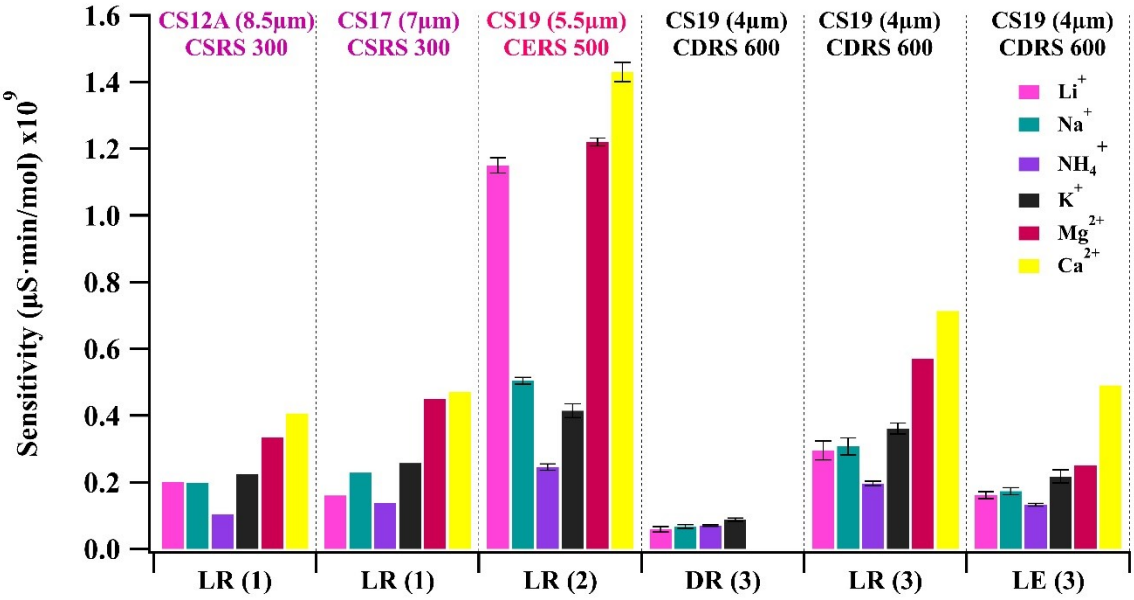

Fig. S7 Sensitivity of inorganic cations by using different cation-exchange columns and suppressors over a decade. The analytes separation and suppression performed by CS12A and CS17 columns, and CSRS 300 in legacy recycle (LR) mode by VandenBoer *et al.* (1);[3] CS19 (5.5 µm), and CERS 500 in LR mode by Place *et al.* (2);[4] and CS19 (4 µm), and CDRS 600 in dynamic recycle (DR), stepped-legacy recycle (LR), and stepped-legacy external (LE) modes in present work (3).

S8. Size-resolved coastal aerosol sample from the marine atmosphere

During the Coastal Fog campaign, nine rounds of aerosol sampling were conducted along the coast of Eastern Canada from September 13 to 24, 2018. Size-resolved atmospheric aerosol samples were collected over the open ocean, the Gulf of the St. Lawrence, and urban harbours. Figure S8 shows the ship track from St. John's, Newfoundland and Labrador to Halifax, Nova Scotia, including indicators for the two sampling sites of the marine and harbour air samples discussed in the main manuscript.

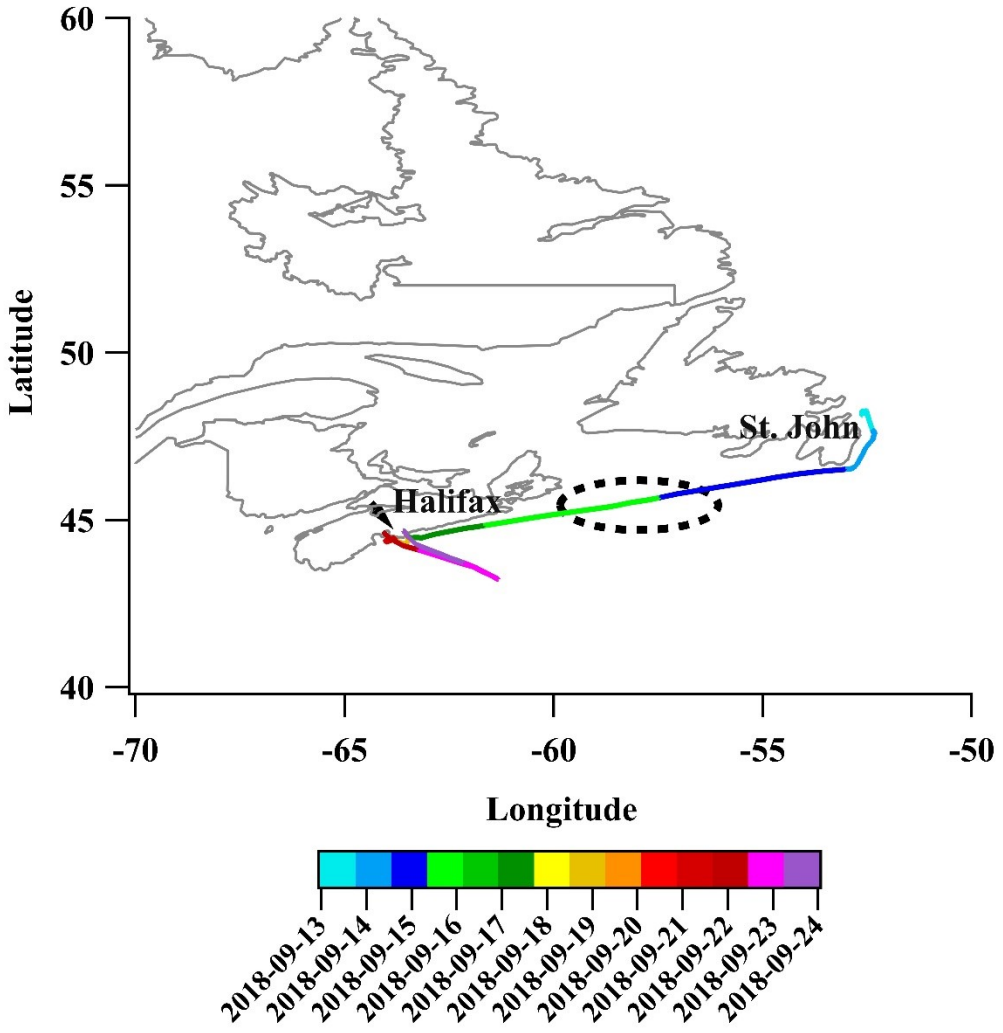

Fig. S8 Coastal FOG ship track from St. John to Halifax along the coast of Eastern Canada from September 13 to 24, 2018. Two MOUDI samples were collected from marine air from 15/09/2018 to 16/09/2018 (dashed black circle), and Halifax harbour air from 18/09/2018 to 19/09/2018 (black arrow) on the Atlantic coast of Nova Scotia, Canada.

S9. Upper Limits on Alkylamine Mixing Ratios in New Home Air Quality Samples

The upper limits of detectable amine mixing ratios were calculated for samples where these were below the detection limit in the NHAQS samples (Table S5). Mixing ratio equivalents (ppbv) were calculated using equation E2 by using the determined detection limits from our method.

$$\text{Mixing Ratio} = \frac{(2\alpha)(LOD)}{Sampling\ time} \quad \text{(E2)}$$

Where 2α (ppbv min ng^{-1}) represents the diffusion coefficient of the NH_3 sampling rate, and instrumental LOD (ng) was obtained from those determined for the stepped-legacy external water mode. Sampling times (min) used were representative of typical sampling durations for this study and many others.[5–7] The α values for alkylamines have not been reported and may differ from those of NH_3, but serve as an initial estimate that we expect to be within a factor of 5 of their true values, based on the relative difference in their gas phase diffusion coefficients, and assuming the same collection efficiency on the citric acid Ogawa reactive pads used.

Table S5: The upper limits of detectable amine mixing ratios were measured in NHAQS, and instrumental LODS were calculated using an optimized method. The diffusion coefficient of NH_3 sampling rate was used at 21 °C (2α= 87), and mixing ratios were determined for two different sampling periods: 1 day (1425 min) and 5 days (5772 min).

Amine	LOD (ng)	Mixing ratio 1day (ppbv)	Mixing ratio 5 days (ppbv)
MEtA	7.99	0.49	0.12
MMA	5.49	0.34	0.08
MEA	9.74	0.59	0.15
DMA	7.90	0.48	0.12
iMPA	21.32	1.30	0.32
MPA	13.39	0.82	0.20
DEA	33.73	2.06	0.51
TMA	16.52	1.01	0.25
MBA	9.70	0.59	0.15
TEA	171.95	10.50	2.59

References

1 S. L. R. Ellison, V. J. Barwick and T. J. Duguid Farrant, *Practical Statistics for the Analytical Scientist*, The Royal Society of Chemistry, UK, 2nd Editio., 2019, vol. 53.

2 F. Raposo, Evaluation of analytical calibration based on least-squares linear regression for instrumental techniques : A tutorial, *Anal. Chem.*, 2016, **77**, 167–185.

3 T. C. VandenBoer, M. Z. Markovic, A. Petroff, M. F. Czar, N. Borduas and J. G. Murphy, Ion chromatographic separation and quantitation of alkyl methylamines and ethylamines in atmospheric gas and particulate matter using preconcentration and suppressed conductivity detection, *J. Chromatogr. A*, 2012, **1252**, 74–83.

4 B. K. Place, A. T. Quilty, R. A. Di Lorenzo, S. E. Ziegler and T. C. VandenBoer, Quantitation of 11 alkylamines in atmospheric samples: Separating structural isomers by ion chromatography, *Atmos. Meas. Tech.*, 2017, **10**, 1061–1078.

5 Ogawa & Co. Inc., NH_3 Sampling Protocol using the Ogawa Sampler, 2017, 1-9. http://ogawausa.com/wp-content/uploads/2017/11/pronh3_1117.pdf

6 M. J. Roadman, J. R. Scudlark, J. J. Meisinger and W. J. Ullman, Validation of Ogawa passive samplers for the determination of gaseous ammonia concentrations in agricultural settings, *Atmos. Environ.*, 2003, **37**, 2317–2325.

7 Z. Y. Meng, W. L. Lin, X. M. Jiang, P. Yan, Y. Wang, Y. M. Zhang, X. F. Jia and X. L. Yu, Characteristics of Atmospheric Ammonia over Beijing, China, *Atmos. Chem. Phys*., 2011, **11**, 6139–6151.